



# Kaolin mining waste to produce geopolymers: Physicomechanical properties and susceptibility to efflorescence formation

Márlon A. Longhi<sup>a,\*</sup>, Erich D. Rodríguez<sup>b</sup>, Zuhua Zhang<sup>c</sup>, Sandro M. Torres<sup>d</sup>, Márcio S. Barata<sup>e</sup>, Ana P. Kirchheim<sup>a</sup>

<sup>a</sup> Department of Civil Engineering, Post-Graduate Program in Civil Engineering: Construction and infrastructure, Universidade Federal do Rio Grande do Sul (NORIE/UFRGS), Porto Alegre, RS, Brazil

<sup>b</sup> Department of Structures and Civil Construction. Center of Technology (CT), Universidade Federal de Santa Maria (UFSM), Santa Maria, RS, Brazil

<sup>c</sup> Key Laboratory for Green & Advanced Civil Engineering Materials and Application Technology of Hunan Province, College of Civil Engineering, Hunan University, Changsha 410082, PR China

<sup>d</sup> Department of Mechanical Engineering, Universidade Federal da Paraíba, João Pessoa, PB, Brazil

<sup>e</sup> Graduate Program in Architecture and Urbanism, Universidade Federal do Pará, Belém, PA, Brazil

## ARTICLE INFO

### Keywords:

Calcinated kaolin  
Mining waste  
Alkali-activated materials  
Geopolymers  
Waste valorization  
Durability

## ABSTRACT

The kaolin mining waste (KW) is a residue generated during the purification process of extracting high purity kaolin used in different industries. KW is mainly constituted by kaolinite-rich clay and other secondary minerals such as anatase and quartz. With the appropriated and controlled process, calcined kaolin mining waste (CKW). It can be thermally activated by calcination to obtain a highly reactive metakaolinite rich material, which exhibits interesting pozzolanic properties. According to its chemical composition and high reactivity, this material is used as an aluminosilicate precursor in the production of geopolymers. One of the negative effects may be the formation of efflorescence. This paper evaluated geopolymer produced with CKW at different activation conditions (alkali concentration and sodium silicate content). The leaching of alkalis was studied through the development of efflorescence on the surface of hardened samples exposed to efflorescence formation conditions (contact with air and water). The results indicated that a larger activator provided a higher compressive strength and reduced the capillary absorption and the efflorescence formation. The data showed that the efflorescence formation can be appropriately controlled by adjusting the mix design parameters, especially the sodium silicate content.

## 1. Introduction

The development of more environmentally friendly cement requires a deeper understanding of its properties for real application on a large scale. One of the promising alternatives is geopolymer or alkali-activated material that is produced by a chemical reaction between aluminosilicate mineral source materials (also called precursor) and a highly alkaline solution (called activator) [1–4]. The most common source materials used as precursors are industrial by-products, such as coal combustion ashes [5–8], granulated blast furnace slag [9,10], and heated clays [11,12]. The main activator is usually based on alkaline hydroxides and silicates solutions.

\* Corresponding author.

E-mail address: [marlonlonghi@gmail.com](mailto:marlonlonghi@gmail.com) (M.A. Longhi).

The obstacles for geopolymer wide application are related to the heterogeneity of precursors, the lack of knowledge of the properties in long service-life, the lack of standards, and the high cost of activators. This heterogeneity is due to the fact that most precursors are based on aluminosilicate-containing by-products from different industries. It is an obstacle, but it is also an advantage because a significant amount of industrial wastes and residues can be valorized by this technology, turning wastes into value-added cement. Thus, there is a direction of research toward evaluating properties, economic and technical applications of locally available materials.

In this context, Brazil is considered the 5th most important mining producer of kaolin. This mineral and its environmental impact is high, considering the vast volume of material beneficiated (1.7–2.0 Mt/y) [13,14]. The purity degree required by the kaolin mining industries generates a high-quality product which is highly desirable by different industries, including ceramics, painting, polymers, among others. However, the mining process is constituted of several stages: centrifugation, magnetic separation, chemical bleaching, and filtration. As a result, it is common to generate a large volume of residues [15] and locally known as kaolin mining waste (KW) and classified as an inorganic residue, inert and non-hazardous material class IIA according to Brazilian standards [16]. Even with the high purity of the main product, the volume of this kaolinite-rich residue is still very large and exhibits potential feasibility for its re-use. Therefore, a controlled thermal treatment is applied. The calcined kaolin waste (CKW) produced at temperatures between 750 and 900 °C eliminates the free water present in the sludge, as well as promotes the dihydroxylation process [17]. This temperature range also promotes a change in the coordination number of aluminium from six to four [18]. The chemical and micro-structural transformation increases the reactivity of these materials to be used as pozzolans or supplementary cementitious material [19], raw material for zeolites synthesis [20], as well as precursor to produce geopolymers [21]. The CKW, when compared to commercial metakaolinite, may show the presence of some impurities (quartz and anatase) and presents a coarser particle size distribution.

Additionally, the most important difference related to precursors is the amount of reactive phases represented by the oxide composition degree. Therefore, the synthesis parameters (alkali type activator, concentration, and water content) and conditions (temperature and time) for its geopolymerization can differ slightly from MK-high reactive precursors. According to the previous study [21], KW can be a feasible aluminosilicate precursor to produce geopolymers; however, these differences for synthesis production affect the mechanical properties, as well as its durability, including efflorescence formation.

Among the factors related to durability, alkali leaching and the potential efflorescence formation are determining factors to be considered [18]. The extremely high alkalinity of activators is necessary to promote the aluminosilicate dissolution and the following geopolymerisation process. The Sodium can be linked to aluminum tetrahedrally coordinated to neutralize the charge of  $\text{Al}(\text{OH})_4$  group [22] partially bounded in the gel structure (higher bounded energy) and associated to molecular water (weaker) [23]. Theoretically, the maximum content of partially bounded alkalis is associated with a unitary ratio with  $\text{Al}_2\text{O}_3$ . The excess of this alkali is present in the porosity of the geopolymer. However, not all aluminum is in a tetrahedral format, which reduces the effectiveness of the alkalis' imprisonment, increasing the leachability potential.

Even though the alkali leaching mechanism has been studied, there is still a need to systematically evaluate such an important factor regarding waste type precursors and durability features. Previous studies identified values of alkali leaching between 1% and 7% using natural pozzolan [24], 12% and 16% using fly ash [25], and values up to 50% using a pure metakaolinite clay [26]. These alkali leaching values depend on synthesis parameters, type of aluminosilicate precursors, time and temperature of curing, and alkali leaching method used. A previous study in MK-based geopolymers indicates a microstructural change associated with Si and Al species in geopolymeric gel associated to alkali leaching [26]. Due to the porosity features of the geopolymers, when exposed to an environment with potential for fluid movement, as well as the free alkalis in the pores can be leached to the surface. In this case, in contact with  $\text{CO}_2$  from the environment, a carbonate species dissolve into the solution at high pH. Some carbonate phases can precipitate within the first surface layer (which has been called as subflorescence) or the growing of an external layer, which is clearly identified

**Table 1**  
Physical properties and chemical composition of calcined kaolin mining waste. LOI is loss of ignition at 950 °C.

		CKW
Physical properties	D <sub>10</sub> (μm)	1.07
	D <sub>50</sub> (μm)	4.42
	D <sub>90</sub> (μm)	31.74
	D <sub>[3,4]</sub> (μm)	10.74
	Specific área (m <sup>2</sup> /g)	21.48
	Density (kg/m <sup>3</sup> )	2630
Chemical composition	Oxide (wt%)	
	SiO <sub>2</sub>	59.16
	Al <sub>2</sub> O <sub>3</sub>	36.94
	TiO <sub>2</sub>	0.73
	Fe <sub>2</sub> O <sub>3</sub>	1.2
	Na <sub>2</sub> O	0.19
	K <sub>2</sub> O	0.07
	CaO	–
	SO <sub>3</sub>	0.38
	P <sub>2</sub> O <sub>5</sub>	0.17
	MgO	
	LOI	1.11

by efflorescence, constituted by a white foamy precipitated [27]. The efflorescence formation depends on the physical properties of geopolymers, synthesis parameters, type of precursors, and activators [25,28–30], and based on its magnitude, a detrimental effect on the mechanical properties can be identified [26]. These previous studies were developed in geopolymers produced with highly reactive commercial MK, and it is still not clear the behavior related to the use of calcined kaolin waste associated with alkali leaching, efflorescence formation, and mechanical behavior after exposure. The different content of silica and alumina, as well as physical features in this material compared to MK may be determining factors associated with efflorescence formation. Therefore, the aim of this paper is to evaluate the alkali leachability and the susceptibility of efflorescence formation in CKW-based geopolymers and its effect on compressive strength, capillary absorption, and some microstructural change.

## 2. Experimental program

### 2.1. Materials and sample preparation

A calcined kaolin mining waste (CKW) from Pará (Brazil) was used as an aluminosilicate precursor. The dried kaolin mining waste was calcinated in a static oven at 750 °C for one hour and mechanically treated in a ball mill, using ceramic balls in a proportion 1:10 (CKW/balls) for one h, according to previous studies [21]. The mineralogical and physical properties and chemical composition (as determined by XRF) are shown in Table 1 and Fig. 1, respectively. In Fig. 1 is visible the phase transformation from kaolin waste (KW), which contains kaolinite, into amorphous CKW. This elucidates that complete áterialaion was not achieved under the thermal conditions assessed here. Compared to the highly reactive commercial MK, which presents a surface area of 13.49 m<sup>2</sup>/g and a mean particle size of 4.56 µm [26], the CKW presents a higher specific surface and coarser particle size, lower content of Al<sub>2</sub>O<sub>3</sub>, and higher content of SiO<sub>2</sub>. Due to the origin of the material and the presence of these crystalline phases, the CKW presents a slightly lower pozzolanic reactivity when compared to the áterial MK. The main crystalline phases observed are Anatase (TiO<sub>2</sub>, Pattern Diffraction File, PDF# 00-021-1272) and kaolinite (Al<sub>2</sub>Si<sub>2</sub>O<sub>5</sub>(OH)<sub>4</sub>, PDF# 01-078-2109). The presence of kaolinite indicates that the calcination process can be improved. The loss of mass also indicates that part of CKW remains in its natural form, which is consistent with the diffractograms, where the presence of remaining kaolinite and anatase in CKW is visible. These differences can influence the dissolution rate and reactivity of precursors, as well as an effect on the extent of the reaction.

Activating solutions were produced using an analytical grade sodium hydroxide (NaOH – 99%) and a sodium silicate with 35.59% of SiO<sub>2</sub>, 15.01% of Na<sub>2</sub>O, and 52,7% of H<sub>2</sub>O. Both were mixed with áter in a specific amount to compose the activator and stored in room áteriala for 24 h. The geopolymers were formulated with different contents of alkali activator (Na<sub>2</sub>O= 10%, 15%, and 20%). The type and content of alkalis were selected according to the áterial [31,32]. Additionally, the same synthesis parameters were used in previous studies [26,28] with commercial MK as the main precursor, allowing the direct comparison between the evaluated properties. The increasing of silica was designed by the addition of sodium silicate in the activator (expressed as Ms modulus, represented by the SiO<sub>2</sub>/M<sub>2</sub>O molar ratio) as 0.0, 0.5, and 1.0. The geopolymer formulations are identified by codes: “Type of precursor – content of alkali – Ms modulus”. The áter/binder (w/b) ratio was fixed at 0.55 for all geopolymers. The pastes were produced by mechanical mixing for 6 min and then poured into molds, vibrated for 1 min and cured at room áteriala (25 ± 2 °C), sealed inside a hermetically sealed box with high relative humidity (~90%), to avoid the loss of áter by evaporation and stored until the day of testing (Table 2).

### 2.2. Tests conducted

The *compressive strength* of each hardened paste was measured at 1, 7, 28, 90 and 360 days, using a universal mechanical testing machine EMIC with a loading speed of 0.5 mm/min. For each geopolymer, before and after efflorescence formation, five cubic samples of 20 mm were tested.

*Determination of leached sodium*, performed with geopolymer, previously milled by hand in an agate mortar. The geopolymers were

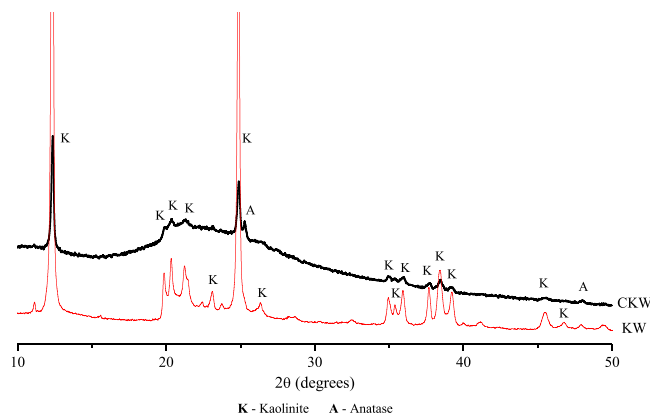


Fig. 1. XRD spectra of CKW used as precursors. K- Kaolinite and A- Anatase.

**Table 2**  
Mix designs of geopolymer samples.

Geopolymers Precursor-%Na <sub>2</sub> O- Ms content	% of Na <sub>2</sub> O	Ms content
CKW – 20 – 1.0	20	1.0
CKW – 20 – 0.5	20	0.5
CKW – 20 – 0.0	20	0.0
CKW – 15 – 1.0	15	1.0
CKW – 15 – 0.5	15	0.5
CKW – 15 – 0.0	15	0.0
CKW – 10 – 1.0	10	1.0
CKW – 10 – 0.5	10	0.5

ground until passed through the 75  $\mu\text{m}$  mesh (# 200 sieve). Then, the samples were placed in a solution with deionized and boiled water to obtain a solid concentration:liquid proportion of 1/100 in sealed PTFE Erlenmeyer áter. The flASKs were stirred for 24 h in constant áteriala shaking incubator. After 24 h of mixing, the solution was neutralized by adding HCl (36 vol%) so that only insoluble phases remained. The neutralized solutions were filtered, and the remaining materials were quantified by mass. The mass difference corresponds to the soluble phases, which are unreacted Na-containing phases (Na(OH), Na<sub>2</sub>O·SiO<sub>2</sub>, as well as sodium carbonates) in the case of geopolymers.

*Capillary water absorption* was quantified using the capillary absorption method, where the dried cylindrical samples  $\Phi 28 \times 55$  mm were partially immersed in 5 mm of water. The amount of absorbed áter was measured every 10 min in the first hour and then every hour to achieve constant mass.

*Quantification of oxide composition after leaching*, performed according to the previous paper, [27], using the process of áter dissolution (WD) and after 28 days of curing. This process consists of removing the soluble material at a pH equal to 7. The process was applied in 2.0 g of grounded geopolymer (passed through a 75  $\mu\text{m}$  sieve) in solution with 200 g of distilled and deionized áter in sealed Erlenmeyer flaskKW. The solution was placed in constant temperature shaking incubator for 5 min, and after that, the pH of the solution was measured and adjusted to a neutral value of pH = 7 through the addition of HCl (36 vol%). This process was repeated until the solution showed a constant pH of 7.0 and the amount of HCl quantified. Then, the solution was filtered using a quantitative filter, then rinsed with distilled áter, and twice with áter (purity of 99%). The remaining solid material was then dried for 45 min in an oven at 40 °C, the chemical composition was assessed by XRF.

*Visual efflorescence formation* was assessed using cylindrical samples with 28 mm of diameter and 55 mm of height after 28 days of curing. The samples were partially immersed in water at 4–5 mm depth at room temperature of  $20 \pm 5$  °C and relative humidity (RH) of  $50 \pm 15\%$  to accelerate the test. Due to the rapid áter absorption and evaporation, the áter level has been adjusted daily.

For each combination evaluates, one cubic áter of 20 mm was crushed and then analyzed by *X-ray diffraction* (XRD) using a D2 Phaser (Bruker) diffractometer with Cu K $\alpha$  radiation ( $\lambda = 1.54178$  Å), with a step size of  $0.02^\circ$ , and a scanning speed of  $0.5^\circ/\text{min}$  for a 2 $\theta$  range of 5–65°.

### 3. Results

#### 3.1. Mechanical and physical properties

The compressive strength results of geopolymers with different synthesis parameters up to 360 days of curing are shown in Fig. 2. The geopolymers produced present values between 7.6 and 52.8 Mpa depending on alkali concentration and soluble silicate content (Ms ratio). Increasing the content of soluble silica in the form of sodium silicate promotes the increment in compressive strength for all Na<sub>2</sub>O concentrations assessed. The higher sodium silicate content tested, Ms = 1 represents an increase in compressive strength up to ~1.5 compared to Ms = 0.5 and ~3.5 compared to Ms = 0. These results are consistent with other studies and associated with formation

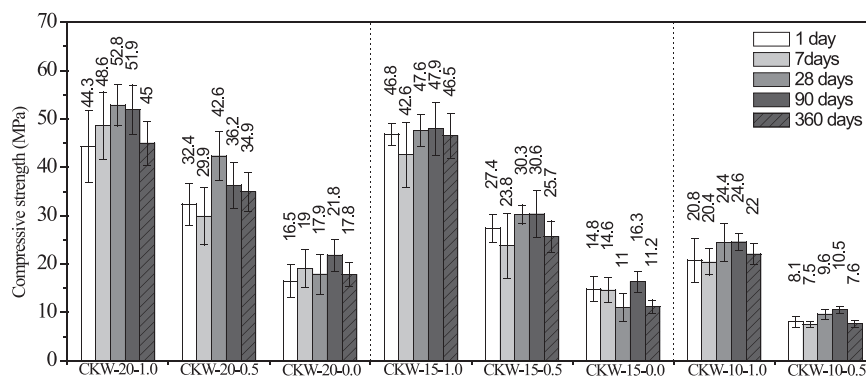


**Fig. 2.** Compressive strength of geopolymers produced at different Na<sub>2</sub>O alkali concentrations and Ms ratio.

of denser and more compact microstructure [6,26,33]. The content of sodium is also a determining factor on mechanical performance, where higher compressive strength is observed in the geopolymers produced at 20% of  $\text{Na}_2\text{O}$ . To higher content of sodium silicate (such as  $M_s=1$ ) the compressive strength for 15% and 20% of  $\text{Na}_2\text{O}$  is statistically similar. In this case, for this precursor, the ideal content of  $\text{Na}_2\text{O}$  is between 15% and 20%. The time of curing is also an important aspect, where at 28 days, an increase in compressive strength is observed, while to later ages ( $\geq 90$ days), a reduction up to 32% can be identified. This reduction is most evident in combination with reduced or no sodium silicate content. The same behavior was also observed in the previous paper [21] and can be associated with the start of zeolite crystallization because of a certain instability from the amorphous reaction products [34,35]. This behavior is also associated to the  $M_s$  content, since the most expressive reductions are observed to geopolymers activated solely with sodium hydroxide. Additional studies are necessary to fully understand this behavior.

Taking into account that the CKW precursor is not produced using a high purity material, it is important to compare the results with arterial high reactive MK-based geopolymers. Using equivalent synthesis parameters (reported in a previous paper, [26]) it is observed

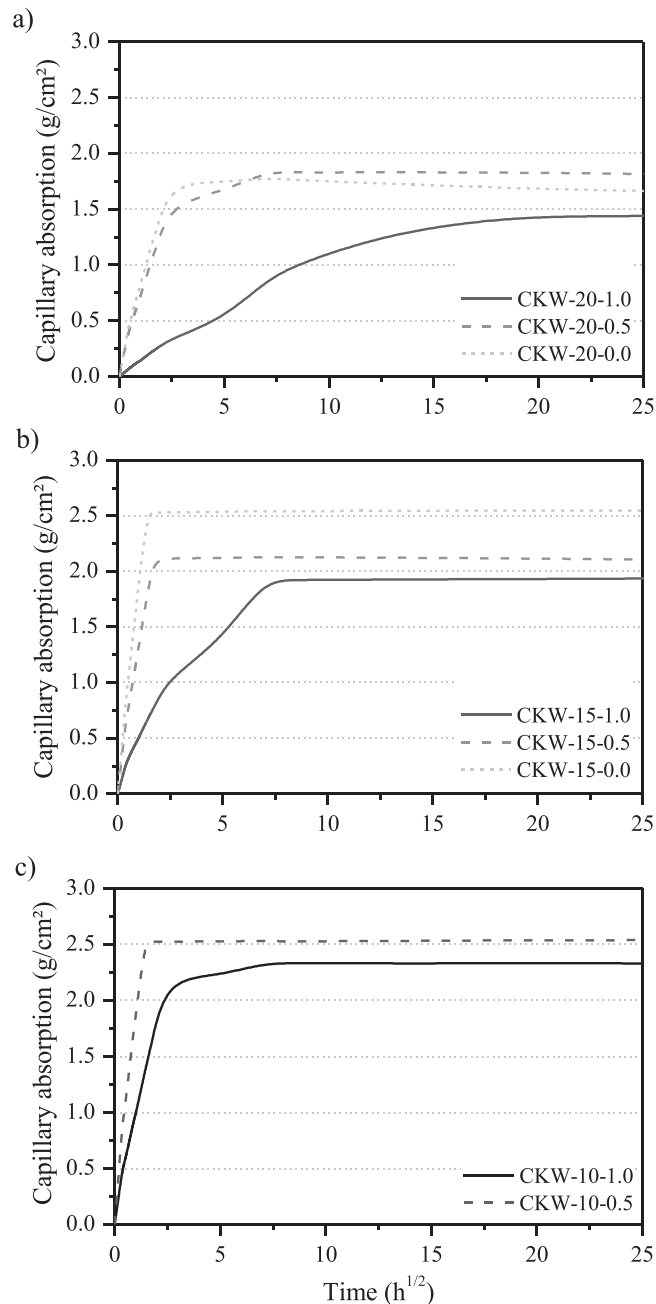


Fig. 3. Capillarity absorption of geopolymers after 28 days of curing.

a compressive strength of 40 Mpa to geopolymers activated at 20% of Na<sub>2</sub>O (MK-20–1.0) and 21.5 to those systems activated at 15% Na<sub>2</sub>O (MK-15-1.0). When these values are compared to CKW-based geopolymers, an increasing up to 1.2 and 2.1 times is observed. The higher compressive strength developed by the CKW geopolymers can be attributed to the oxide composition of this precursor, where the presence of higher SiO<sub>2</sub>/Al<sub>2</sub>O<sub>3</sub> ratio associated to the use of CKW can increase the presence of Si-rich Q<sup>4</sup> sites rich due to the high degree of polymerization [6]. This expressive improvement can also be related to the amount of metakaolinite present in the CKW used, related to the high amount of kaolinite present in the kaolin mining waste, at approximately 92%, as reported previously [21]. The use of CKW is effective even in the absence of a thermal curing process during geopolymer production, which facilitates the use of material for different applications and reduces the cost and CO<sub>2</sub> emissions.

Additionally, to compressive strength results, Fig. 3 shows the capillary water absorption for all samples. The geopolymer produced at lower Na<sub>2</sub>O content presents a short time until the saturation point. The same behavior is observed in systems with low amount of sodium silicate (Ms ratio of 0 and 0.5), which make these systems more susceptible to mass change by water transportation. As an example, the system CKW-20–1.0 presents a saturation point approximately after 14 days, while CKW-10–1.0, at 2 days. The highest saturation point is identified for the system with 20% of Na<sub>2</sub>O and Ms = 1.0. Similar behavior is observed to the amount of water absorbed, where higher amount of alkali and high amount of SS reduces the water absorption, where CKW-20–1.0 presents approximately 1.5 g/cm<sup>2</sup> at 28 days, while CKW-10–0.5 shows ~2.5 g/cm<sup>2</sup>. The behavior observed in each system can be correlated directly to leaching and potential efflorescence formation and will be discussed in more detail in the following sections. As expected, lower capillarity absorption is aligned to higher compressive strength. This behavior is associated to synthesis parameters, where the addition of higher content of sodium allows a greater extent of reaction [36] and the addition of sodium silicate, the formation of a microstructure with more bounded Si in Q<sup>4</sup>(1Al) and Q<sup>4</sup>(2Al) sites, providing a stronger network structure [23].

### 3.2. Leaching potential

#### 3.2.1. Sodium containing phases leachability

The results of this procedure are presented in Table 3. The total loss of mass is higher when a greater amount of alkali is used for the activation. However, the percentage of alkali leached, relative to the initial amount required (or included during the activation), is higher to geopolymer systems with a lower amount of sodium, indicating an inefficient geopolymerisation and high percentage of free alkalis in the pore solution. The values of total loss are consistent with those reported previously [26]. The addition of sodium silicate is the major parameter associated with reduction in alkali leaching. The higher extent of reaction and the type of Q<sup>4</sup>(mAl) structure is associated to its use [6]. Consequently, a higher amount of Al(IV). In this case, a higher amount of Na<sup>+</sup> is required to establish an equilibrium in charge balancing associated to aluminum [31]. It is important to note that the mass of loss for each system is similar to the content of sodium used, however, just a fraction of this sodium is leached, indicating the dissolution of different oxides. In the same way, not leached sodium is stable in the framework structure.

#### 3.2.2. Effects of leachability on oxide composition

A selective dissolution process was developed previously in a study to determine the content of soluble materials at neutral pH and the content of gel formed in MK-based geopolymers [26]. This procedure was also used here to determine the content of leachable materials in a neutral pH to correlate with efflorescence formation and the consequent damaging effect in compressive strength. According to the procedure used, the geopolymer sample is reduced to powder and exposed to a severe condition, which can be more damaging than under use condition. The results showed represent the maximum potential of leaching and are valid just for the specific exposed conditions. In Table 4 are shown the results of oxide composition, where the geopolymers present an expressive loss of mass associated to leaching of free oxides or soluble phases. The main reduction is associated to the leachability of Na<sub>2</sub>O, demonstrating that part of the activator is free in the pore solution or weakly bonded from the reaction products [26]. This fraction is higher in systems with a lower amount of sodium silicate.

#### 3.2.3. Relation between oxides composition, alkali leaching and compressive strength

The combined data of oxide composition determined before leaching (Table 3) by XRF with the quantification of leached alkali (Table 4) as well as compressive strength data (Fig. 2) are presented in Fig. 4, where it is possible to place the systems within a ternary diagram SiO<sub>2</sub>-Al<sub>2</sub>O<sub>3</sub>-Na<sub>2</sub>O. It is evident that the lowest leaching values are observed in systems where there is a balance between the oxides. Insufficient amount of Na<sub>2</sub>O in the activator does not allow the complete reaction of the precursor, consequently, a lower

**Table 3**  
Loss of mass and sodium leached in a neutral environment.

Geopolymer	Initial pH	Loss of mass (%)	HCl consumption (g)	Sodium containing phases leached (%)
CKW - 20–1.0	10.70	17.8	0.065	11
CKW - 20–0.5	10.95	20.1	0.100	17
CKW - 20–0.0	10.54	20.2	0.134	23
CKW - 15–1.0	10.79	15.4	0.092	21
CKW - 15–0.5	10.82	16.8	0.113	25
CKW - 15–0.0	10.74	16.8	0.142	32
CKW - 10–1.0	10.63	13.3	0.121	41
CKW - 10–0.5	10.6	14.2	0.121	41

**Table 4**  
Oxide composition before and after selective dissolution in neutral condition.

Geopolymer	Initial condition (%)			After dissolution in neutral pH (%)		
	SiO <sub>2</sub>	Al <sub>2</sub> O <sub>3</sub>	Na <sub>2</sub> O	SiO <sub>2</sub>	Al <sub>2</sub> O <sub>3</sub>	Na <sub>2</sub> O
CKW - 20-1.0	68.9	12.7	16.8	70.1	16.9	11.5
CKW - 20-0.5	65.4	14.2	18.2	67.5	19.0	14.1
CKW - 20-0.0	60.4	16.0	21.0	65.0	21.4	12.0
CKW - 15-1.0	70.2	15.3	13.0	71.5	18.8	8.4
CKW - 15-0.5	67.2	16.5	14.7	69.2	19.9	9.6
CKW - 15-0.0	64.6	17.5	16.3	68.2	22.1	8.0
CKW - 10-1.0	70.7	17.2	10.6	72.9	20.0	5.6
CKW - 10-0.5	69.7	17.8	10.9	71.2	20.9	6.4

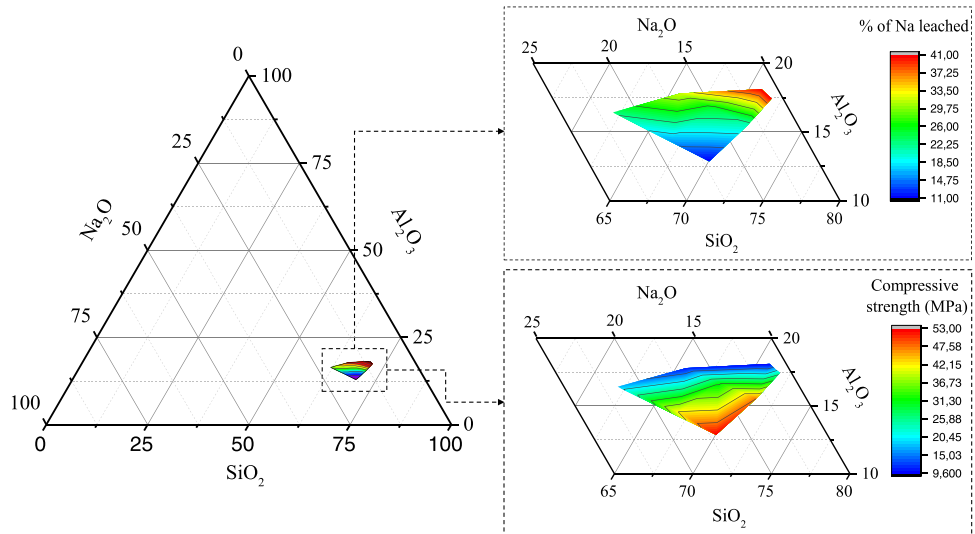


Fig. 4. Geopolymer situated in a ternary diagram and associated with leaching potential and compressive strength.

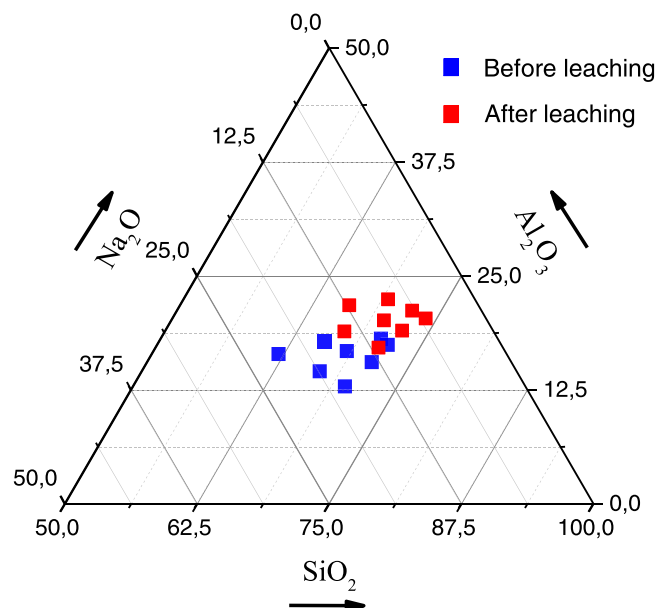


Fig. 5. Ternary diagram of geopolymers oxides (SiO<sub>2</sub>, Al<sub>2</sub>O<sub>3</sub>, and Na<sub>2</sub>O).

amount of gel is formed, and alkali leachability is increased. Under designed geopolymer tested, the leachability is more pronounced associated to the lower amount of  $\text{Na}_2\text{O}$  and higher  $\text{Al}_2\text{O}_3$ , characteristic to systems without the addition of sodium silicate. The region with the lowest amount of leachable materials is the same with higher compressive strength, which is consistent with a higher amount of gel formed and a denser structure.

As the composition of oxides was also evaluated after exposure to leaching conditions, it is possible to verify the alteration of such composition in a ternary diagram. Evaluating just the three main oxides, in Fig. 5, it is easy to identify the shift of the chemical composition assemble to higher  $\text{Al}_2\text{O}_3$  content. This change does not mean an increase in these oxides content but a proportional adjustment to compensate the excessive loss of alkalis. The loss of alkali is clear during leaching evaluation. The content of alumina seems to increase, while the content of silica seems stable. However, the increase in aluminate is just proportional to compensate the loss of other oxides. This result is important to confirm the stability of the geopolymeric gel. However, analyzing the  $\text{SiO}_2/\text{Al}_2\text{O}_3$  ratio before and after dissolution, it is possible to observe a reduction in this value, indicating a partial removal of silica. This change may be related to a possible unstable removal or not well-formed phases of geopolymeric gel. Even in a neutral pH, the removal of alkalis may present nanostructural changes associated to the reduction of  $\text{Q}^4(4\text{Al})$  and  $\text{Al}(\text{IV})$  species as observed by  $^{29}\text{Si}$  Mas NMR and  $^{27}\text{Al}$  Mas NMR, respectively [26]. In this case, a fraction of the silicate gel can be leached in a neutral pH; however, this hypothesis requires further studies. However, due to the stability of  $\text{Al}_2\text{O}_3$  content, the removal of sodium is more probable to be associated with the removal of silicate monomers formed during the geopolymerization process.

### 3.3. Susceptibility to efflorescence formation

The evolution of efflorescence formation up to 28 days in cylindrical samples immersed partially in water is shown in Fig. 6. Several samples present efflorescence formation within the period of time assessed; however, in some geopolymers, this formation is not observed clearly. The presence of efflorescence is more pronounced in systems with a low amount of sodium silicate (or  $\text{Ms}=0.5$  and  $\text{Ms}=0.0$ ) compared to geopolymers with a high amount of sodium silicate (such as  $\text{Ms}=1.0$ ). Regardless to the content of sodium, by images, it is not clear and possible to conclude which content presents the best behavior, however by visual observation, the content of 20% shows minor superficial damage. The geopolymer with the best behavior (or lowest efflorescence formation) was produced with 20% of  $\text{Na}_2\text{O}$  and  $\text{Ms}=1.0$ .

As observed in compressive strength, capillary absorption, and alkali leaching, all these properties are dependent on synthesis

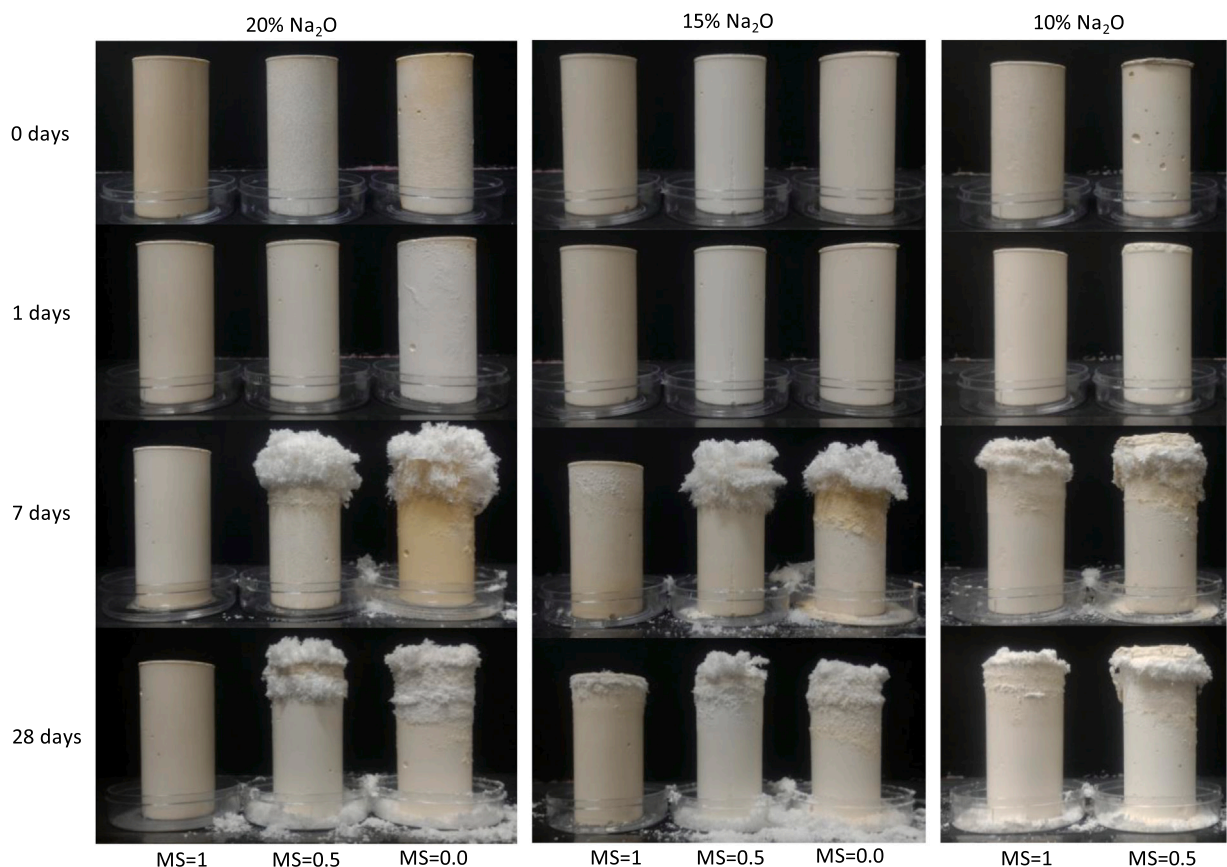


Fig. 6. evolution of efflorescence formation during 28 days of exposure in geopolymer samples partially immersed in water.

parameters. In the same way, these properties are associated to efflorescence formation. These two main factors are associated to potential of alkali leaching and its transport through the pore network. In geopolymers, the main mechanism of transport is the capillary pressure. In this situation, wetting and drying cycles allow the liquid movement of water and soluble material from the internal part of the sample to the surface. In geopolymers with a higher potential of leaching, a greater amount of sodium released can be identified on the surface, and consequently, more severe is the efflorescence formation. Thus, the results reported here are consistent, and the higher extent of efflorescence formation is observed in geopolymers with higher water absorption and higher leaching potential.

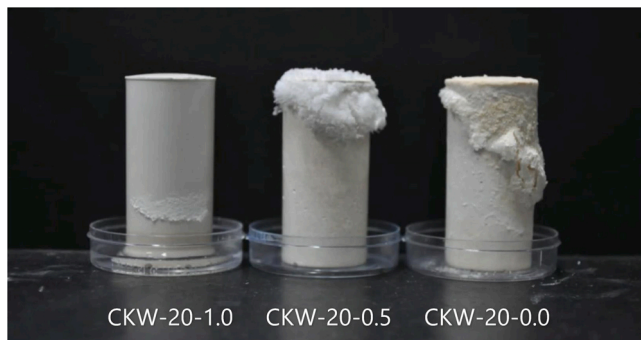
Compared to a previous study [37], when using the same formulation of activator to produce highly reactive MK-based geopolymers, the use of CKW seems to be more effective than MK by reason of the absence of efflorescence formation in some systems (especially those with higher amount of SS). Especially to the geopolymer with high amount of sodium silicate, the content of leachable sodium is inferior than the one in the referred paper. This behavior can be associated to a higher amount of  $\text{SiO}_2$ , which allows the formation of a framework structure rich in Si and consequently the formation of a denser structure.

Usually, the efflorescence formation is reported by images in a specific period of exposure. This type of analysis is useful; however, the behavior associated to absorption, water transport, and efflorescence formation has not been assessed in real-time. In order to clarify this behavior, a time-lapse video (Video 1) recording the first 24 h of exposure is shown. In this video, the efflorescence formation in the geopolymers CKW – 20 – 1.0, CKW – 20 – 0.5, CKW – 20 – 0.0 has been recorded. The rate of absorption is consistent with the results presented in Fig. 3, where higher values of initial water absorption allow a faster transportation of water and leached alkalis. Consequently, the efflorescence formation is anticipated in these systems.

In order to understand the product formed during the efflorescence formation, the X-ray diffractograms of geopolymers and the efflorescence product are shown in Fig. 7. The CKW presents an evident amorphous hump between  $15^\circ$  and  $30^\circ$   $2\theta$ , indicating a proper material to be used as precursor (Fig. 1). After geopolymerisation process, traces of anatase, kaolinite, and quartz are still observed in all systems. It is also important to note the presence of zeolite A ( $\text{Na}_{96}\text{Al}_{96}\text{Si}_{96}\text{O}_{384}\cdot 261\text{H}_2\text{O}$ , PDF# 00-039-0272) in the geopolymer with  $M_s = 0.0$ . This phase was observed previously in MK-based geopolymer [11,37,38,39] and reported as a product formed in metakaolinite-based geopolymers produced with sodium hydroxide (without silicate soluble in the activator solution). The other important product observed in geopolymer systems is associated to efflorescence product, which is more evident in geopolymer CKW-20-0.0, without sodium silicate as activator, and consistent with visual efflorescence formation and alkali leaching. It is important to consider that the peak related to this phase is not so intense due to small amount of efflorescence compared to the volume of the sample. In this sense, the Fig. 7A shows the XRD for the white powder (or efflorescence product) collected on the surface of the damaged sample. The main phases observed in this leached/precipitated product are sodium carbonate ( $\text{Na}_2\text{CO}_3$ , PDF# 01-086-0301) and hydrated sodium carbonate ( $\text{Na}_2\text{CO}_3\cdot\text{H}_2\text{O}$ , PDF# 01-070-2148). These products were also identified in the geopolymer sample but with a lower intensity (mainly to the geopolymer CKW-20-0.0). The same products were also reported in other studies [22,34–36].

### 3.4. Effect of efflorescence formation in mechanical properties

After a severe efflorescence formation in some samples, and with potential damaging associated to this phenomenon reported in previous papers [25,27], it is necessary to evaluate the compressive strength after exposure conditions for CKW-based geopolymers. According to these studies, efflorescence formation induces the formation of the carbonate, which can cause an internal stress and affect their mechanical properties. Additionally, another fact that can contribute to the damaging is the development of subflorescence [27], a crystallization in the first superficial layer of the geopolymer. The results after 7, 14, and 28 days of exposure are shown in Fig. 8, and are consistent with those reported in the literature, where the presence of visual efflorescence formation can damage the



**Video 1.** Time-lapse video of 24 h exposure of geopolymeric samples to water in the bottom to allow the efflorescence formation. A video clip is available online. Supplementary material related to this article can be found online at [doi:10.1016/j.cscm.2021.e00846](https://doi.org/10.1016/j.cscm.2021.e00846).

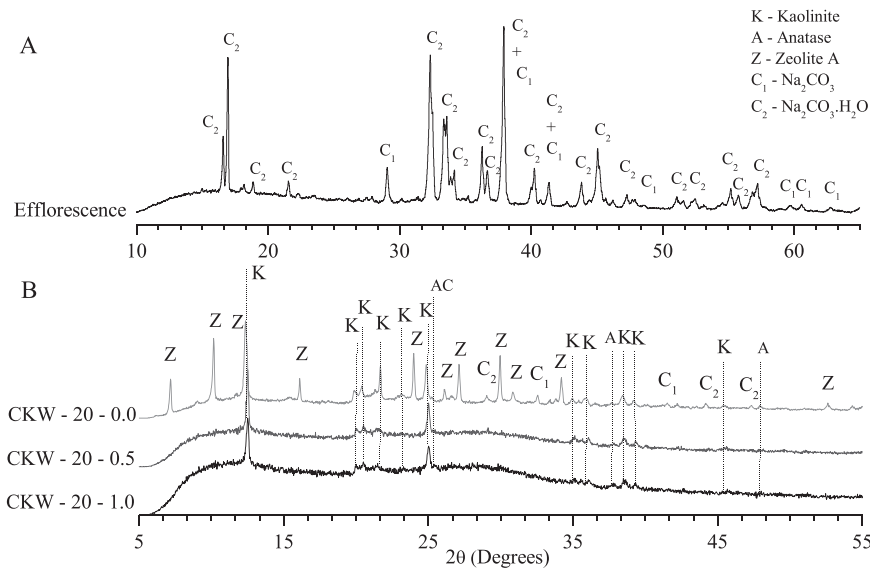


Fig. 7. XRD analysis A – Efflorescence product, B - geopolymers after efflorescence formation.

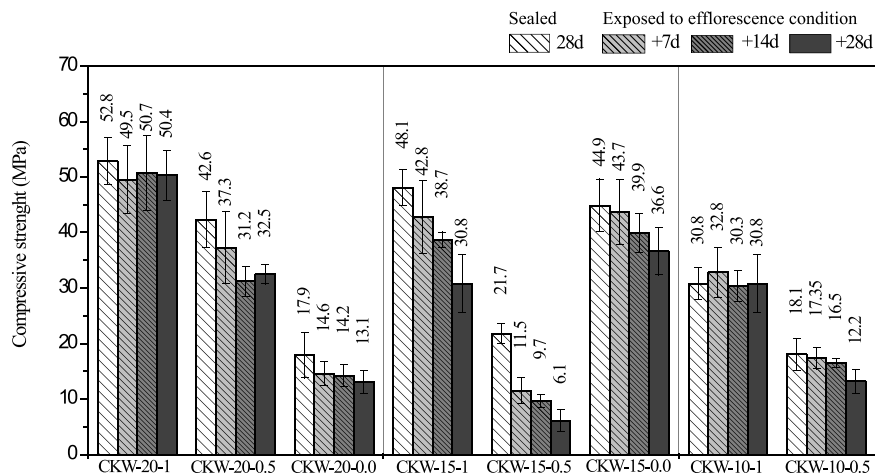


Fig. 8. Compressive strength of geopolymers after exposure to efflorescence formation.

sample and reduce the mechanical strength [28,29,40]. When exposed to efflorescence formation, geopolymers produced with Ms= 1 do not reduce the compressive strength (< 5%), while geopolymers with Ms= 0.5 and 0.0 can present a reduction up to 65% after 28 days of exposure. The content of sodium does not influence directly the behavior associated to the reduction in compressive strength, while the content of sodium silicate is the most important factor. Time is also an important factor. A longer period of exposure can increase the deterioration, which is consistent and aligned to alkalis removal observed in Fig. 3. The deterioration under efflorescence conditions can be associated to the excessive carbonate crystallization and internal stress caused [29]. The intensity of this crystallization is associated to the amount of leachable alkalis and porosity. This crystallization process is associated to the equilibrium relative humidity of each type of carbonates [18], which means that the crystallization starts in a specific humidity for each type of carbonate. As observed in Fig. 7, the carbonate phases are sodium carbonate and hydrated sodium carbonate, and under tested conditions, the equilibrium humidity is reached. However, additional studies are necessary to identify the humidity and the crystallization pressure caused. The mechanical behavior and the leaching of alkalis and aluminosilicates observed in leaching tests indicate a potential damaging process associated with geopolymers, which can limit the applications under certain conditions.

#### 4. Conclusions

This study demonstrates that calcined kaolin mining waste is a potential material to be used as a precursor for geopolymer production. The compressive strength observed is consistent and even higher compared to metakaolin-based geopolymers. This property,

as well as capillary water absorption, is dependent on design parameters, where higher amount of activator and sodium silicate provides the most resistant and less porous materials. Sodium silicate accelerates and increases the geopolymerization degree of CKW particles.

In order to access the leaching and efflorescence potential of geopolymers produced, it was observed an extensive degree of dissolution, related specifically to the dissolution of sodium and some soluble silicate phases. The leaching potential, associated to capillary absorption, allows the efflorescence formation in different levels. The extensive efflorescence formation can reduce the compressive strength. However, this effect can be mitigated by using appropriated synthesis parameters. The results found were, demonstrate potential leaching and efflorescence formation and are consistent to other studies using metakaolin as precursors or even better in compressive strength, which makes the CKW a promising precursor to geopolymers.

## Funding

M.A. Longhi is grateful for the financial support of CAPES and of SWE 203750/2017-9. The participation of A. P. Kirchheim Brazilian authors was sponsored by CNPq (Brazilian National Council for Scientific and Technological Development) through the research fellowships PQ2017 305530/2017-8. The participation of E. D. Rodríguez was supported by CNPq research fellowship PQ 309885/2020-5, and 49992/2018-6. The participation of Z. Zhang was supported by National Scientific Foundation of China (51878263, U2001225 and 51638008).

## Declaration of Competing Interest

The authors declare that they have no known competing financial interests or personal relationships that could have appeared to influence the work reported in this paper.

## References

- [1] J.L. Provis, Alkali-activated materials, *Cem. Concr. Res.* (2018), <https://doi.org/10.1016/j.cemconres.2017.02.009>.
- [2] J.S.J.J. van Deventer, J.L. Provis, P. Duxson, Technical and commercial progress in the adoption of geopolymer cement, *Miner. Eng.* 29 (2012) 89–104, <https://doi.org/10.1016/j.mineng.2011.09.009>.
- [3] J.L. Provis, S. a Bernal, Geopolymers and related alkali-activated materials, *Annu. Rev. Mater. Res.* 44 (2014), 140205180727009, <https://doi.org/10.1146/annurev-matsci-070813-113515>.
- [4] P. Duxson, A. Fernández-Jiménez, J.L. Provis, G.C. Lukey, A. Palomo, J.S.J. Deventer, Geopolymer technology: the current state of the art, *J. Mater. Sci.* 42 (2006) 2917–2933, <https://doi.org/10.1007/s10853-006-0637-z>.
- [5] M. Criado, A. Fernández-Jiménez, A. Palomo, Alkali activation of fly ash: effect of the SiO<sub>2</sub>/Na<sub>2</sub>O ratio, *Microporous Mesoporous Mater.* 106 (2007) 180–191, <https://doi.org/10.1016/j.micromeso.2007.02.055>.
- [6] M. Criado, A. Fernández-Jiménez, A. Palomo, I. Sobrados, J. Sanz, Effect of the SiO<sub>2</sub>/Na<sub>2</sub>O ratio on the alkali activation of fly ash. Part II: 29Si MAS NMR Survey, *Microporous Mesoporous Mater.* 109 (2008) 525–534, <https://doi.org/10.1016/j.micromeso.2007.05.062>.
- [7] Y. Rifaai, A. Yahia, A. Mostafa, S. Aggoun, E.H. Kadri, Rheology of fly ash-based geopolymer: effect of NaOH concentration, *Constr. Build. Mater.* 223 (2019) 583–594, <https://doi.org/10.1016/j.conbuildmat.2019.07.028>.
- [8] A.M. Rashad, A comprehensive overview about the influence of different admixtures and additives on the properties of alkali-activated fly ash, *Mater. Des.* 53 (2014) 1005–1025, <https://doi.org/10.1016/j.matdes.2013.07.074>.
- [9] F. Puertas, B. González-Fontbea, I. González-Taboada, M.M. Alonso, M. Torres-Carraso, G. Rojo, F. Martínez-Abella, Alkali-activated slag concrete: fresh and hardened behaviour, *Cem. Concr. Compos.* 85 (2018) 22–31, <https://doi.org/10.1016/j.cemconcomp.2017.10.003>.
- [10] A.M. Rashad, A comprehensive overview about the influence of different additives on the properties of alkali-activated slag - a guide for Civil Engineer, *Constr. Build. Mater.* 47 (2013) 29–55, <https://doi.org/10.1016/j.conbuildmat.2013.04.011>.
- [11] Z. Zhang, H. Wang, J.L. Provis, F. Bullen, A. Reid, Y. Zhu, Quantitative kinetic and structural analysis of geopolymers. Part 1. The activation of metakaolin with sodium hydroxide, *Thermochim. Acta* 539 (2012) 23–33, <https://doi.org/10.1016/j.tca.2012.03.021>.
- [12] A.M. Rashad, Alkali-activated metakaolin: a short guide for civil engineer-an overview, *Constr. Build. Mater.* 41 (2013) 751–765, <https://doi.org/10.1016/j.conbuildmat.2012.12.030>.
- [13] USGS, Mineral Commodity Summaries, (2019).
- [14] M.S. Barata, R.S. Angélica, Caracterização dos resíduos caulínicos das indústrias de mineração de caulim da amazônia como matéria-prima para produção de pozolanas de alta reatividade (Characterization of kaolin wastes from kaolin mining industry), *Cerâmica* 58 (2012) 36–42.
- [15] M.S. Barata, R.S. Angélica, Pozzolanic activity of kaolin wastes from kaolin mining industry from the amazon region, *Matéria* 16 (2011) 795–810.
- [16] A.B. de N.T. ABNT, ABNT NBR10004/2004: Classificação de Resíduos Sólidos (Solid waste - Classification), (2004).
- [17] N. Garg, J. Skibsted, Thermal activation of a pure montmorillonite clay and its reactivity in cementitious systems, *J. Phys. Chem. C* 118 (2014) 11464–11477, <https://doi.org/10.1021/jp502529d>.
- [18] M.A.M.A. Longhi, Z. Zhang, E.D.E.D. Rodríguez, A.P.A.P. Kirchheim, H. Wang, Efflorescence of alkali-activated cements (Geopolymers) and the impacts on material structures: a critical analysis, *Front. Mater.* 6 (2019) 1–13, <https://doi.org/10.3389/fmats.2019.00089>.
- [19] A.A.B. Maia, E. Saldanha, R.S. Angélica, C.A.G. Souza, R.F. Neves, The use of kaolin wastes from the Amazon region on the synthesis of zeolite A, *Cerâmica* 53 (2007) 319–324, <https://doi.org/10.1590/S0366-69132007000300017>.
- [20] A.A.B. Maia, R.S. Angélica, R.F. Neves, Use of industrial kaolin waste from the Brazilian Amazon region for synthesis of zeolite A, *Clay Miner.* 46 (2011) 127–136, <https://doi.org/10.1180/claymin.2011.046.1.127>.
- [21] M.A.M.A. Longhi, E.D.E.D. Rodríguez, S.A.S.A. Bernal, J.L.J.L. Provis, A.P. Kirchheim, Valorisation of a kaolin mining waste for the production of geopolymers, *J. Clean. Prod.* 115 (2016) 265–272, <https://doi.org/10.1016/j.jclepro.2015.12.011>.
- [22] P. Duxson, J.L. Provis, G.C. Lukey, F. Separovic, J.S.J. van Deventer, Si NMR study of structural ordering in aluminosilicate geopolymer gels, (2005), pp. 3028–3036. (<https://doi.org/10.1021/la047336x>).
- [23] A. Fernández-Jiménez, a Palomo, I. Sobrados, J. Sanz, The role played by the reactive alumina content in the alkaline activation of fly ashes, *Microporous Mesoporous Mater.* 91 (2006) 111–119, <https://doi.org/10.1016/j.micromeso.2005.11.015>.
- [24] E. Najafi, A. Allahverdi, J.L. Provis, Efflorescence control in geopolymer binders based on natural pozzolan.pdf, 34, (2012), pp. 25–33. (<https://doi.org/10.1016/j.cemconcomp.2011.07.007>).
- [25] Z. Zhang, J.L. Provis, A. Reid, H. Wang, Fly ash-based geopolymers: the relationship between composition, pore structure and efflorescence, *Cem. Concr. Res.* 64 (2014) 30–41, <https://doi.org/10.1016/j.cemconres.2014.06.004>.

- [26] M.A. Longhi, B. Walkley, E.D. Rodríguez, A.P. Kirchheim, Z. Zhang, H. Wang, New selective dissolution process to quantify reaction extent and product stability in metakaolin-based geopolymers, *Compos. Part B Eng.* 176 (2019), 107172, <https://doi.org/10.1016/j.compositesb.2019.107172>.
- [27] Z. Zhang, J.L. Provis, X. Ma, A. Reid, H. Wang, Efflorescence and subflorescence induced microstructural and mechanical evolution in fly ash-based geopolymers, *Cem. Concr. Compos.* 92 (2018) 165–177, <https://doi.org/10.1016/j.cemconcomp.2018.06.010>.
- [28] M.A. Longhi, E.D. Rodríguez, B. Walkley, Z. Zhang, A.P. Kirchheim, Metakaolin-based geopolymers: relation between efflorescence formation, design parameters and physicochemical properties, Thesis Chapter 5, (2019).
- [29] X. Yao, T. Yang, Z. Zhang, Compressive strength development and shrinkage of alkali-activated fly ash–slag blends associated with efflorescence, *Mater. Struct. Mater. Constr.* 49 (2016) 2907–2918, <https://doi.org/10.1617/s11527-015-0694-3>.
- [30] S.-P. Kang, S.-J. Kwon, Effects of red mud and Alkali-Activated Slag Cement on efflorescence in cement mortar, *Constr. Build. Mater.* 133 (2017) 459–467, <https://doi.org/10.1016/j.conbuildmat.2016.12.123>.
- [31] B. Walkley, G.J. Rees, R.S. Nicolas, J.S.J. van Deventer, J. v Hanna, J.L. Provis, New structural model of hydrous sodium aluminosilicate gels and the role of charge-balancing extra-framework Al, *J. Phys. Chem. C* 4 (2018) 5673–5685, <https://doi.org/10.1021/acs.jpcc.8b00259>.
- [32] Z. Zhang, X. Yao, H. Zhu, Potential application of geopolymers as protection coatings for marine concrete I. Basic properties, *Appl. Clay Sci.* 49 (2010) 1–6, <https://doi.org/10.1016/j.clay.2010.01.014>.
- [33] Z. Zhang, J.L. Provis, H. Wang, F. Bullen, A. Reid, Quantitative kinetic and structural analysis of geopolymers. Part 2. Thermodynamics of sodium silicate activation of metakaolin, *Thermochim. Acta* 565 (2013) 163–171, <https://doi.org/10.1016/j.tca.2013.01.040>.
- [34] P. de Silva, K. Sagoe-Crenstil, V. Sirivivatnanon, Kinetics of geopolymerization: role of Al<sub>2</sub>O<sub>3</sub> and SiO<sub>2</sub>, *Cem. Concr. Res.* 37 (2007) 512–518, <https://doi.org/10.1016/j.cemconres.2007.01.003>.
- [35] H. Takeda, S. Hashimoto, H. Yokoyama, S. Honda, Y. Iwamoto, Characterization of zeolite in zeolite-geopolymer hybrid bulk materials derived from kaolinitic clays, *Materials* 6 (2013) 1767–1778, <https://doi.org/10.3390/ma6051767>.
- [36] K. Gao, K.-L. Lin, D. Wang, C.-L. Hwang, H.-S. Shiu, Y.-M. Chang, T.-W. Cheng, Effects SiO<sub>2</sub>/Na<sub>2</sub>O molar ratio on mechanical properties and the microstructure of nano-SiO<sub>2</sub> metakaolin-based geopolymers, *Constr. Build. Mater.* 53 (2014) 503–510, <https://doi.org/10.1016/j.conbuildmat.2013.12.003>.
- [37] M.A.M.A. Longhi, E.D.E.D. Rodríguez, B. Walkley, Z. Zhang, A.P.A.P. Kirchheim, Metakaolin-based geopolymers: relation between formulation, physicochemical properties and efflorescence formation, *Compos. Part B Eng.* 182 (2020), <https://doi.org/10.1016/j.compositesb.2019.107671>.
- [38] O. Burciaga-Díaz, J.I. Escalante-García, R. Arellano-Aguilar, A. Gorokhovskiy, Statistical analysis of strength development as a function of various parameters on activated metakaolin/slag cements, *J. Am. Ceram. Soc.* 93 (2010) 541–547, <https://doi.org/10.1111/j.1551-2916.2009.03414.x>.
- [39] F. Škvára, L. Kopecký, L. Myšková, V.Í.T. Šmilauer, L. Alberovská, L. Vinšová, Aluminosilicate polymers - influence of elevated temperatures, efflorescence, *Ceram. Silik.* 53 (2009) 276–282.
- [40] L. Srinivasamurthy, V.S. Chevali, Z. Zhang, H. Wang, Phase changes under efflorescence in alkali activated materials with mixed activators, *Constr. Build. Mater.* 283 (2021), 122678, <https://doi.org/10.1016/j.conbuildmat.2021.122678>.